Evidence of non-extensivity in the evolution of seismicity along the San Andreas Fault, California, USA: An approach based on Tsallis statistical physics.

Angeliki Efstathiou & **Andreas Tzanis**

National and Kapodistrian University of Athens,
Department of Geophysics and Geothermy,
Panepistimiopoli, Zografou 15784, Greece;
e-mail: aefstathiou@geol.uoa.gr; atzanis@geol.uoa.gr.

Filippos Vallianatos

Laboratory of Geophysics and Seismology,
Technological Educational Institute of Crete,
Chania, GR 73133, Crete, Greece.
e-mail: fvallian@chania.teicrete.gr

Published in: Physic and Chemistry of the Earth, Parts A/B/C, **85–86**, 56–68, 2015; doi:10.1016/j.pce.2015.02.013.

April 2015

Abstract

We examine the nature of the seismogenetic system along the San Andreas Fault (SAF), California, USA, by searching for evidence of complexity and non-extensivity in the earthquake record. We use accurate, complete and homogeneous earthquake catalogues in which aftershocks are included (raw catalogues), or have been removed by a stochastic declustering procedure (declustered catalogues). On the basis of Non-Extensive Statistical Physics (NESP), which generalizes the Boltzmann-Gibbs formalism to non-equilibrating (complex) systems, we investigate whether earthquakes are generated by an extensive self-excited Poisson process or by a non-extensive complex process. We examine bivariate cumulative frequency distributions of earthquake magnitudes and interevent times and determine the size and time dependence of the respective magnitude and temporal entropic indices, which indicate the level on non-equilibrium (correlation). It is shown that the magnitude entropic index is very stable and corresponds to proxy *b*-values that are *remarkably* consistent with the *b*-values computed by conventional means. The temporal entropic index computed from the raw catalogues indicate moderately to highly correlated states during the aftershock sequences of large earthquakes, progressing to quasi-uncorrelated states as these die out and before the next large event. Conversely, the analysis of the declustered catalogues shows that background seismicity exhibits moderate to high correlation that varies significantly albeit *smoothly* with time. This indicates a *persistent* sub-extensive seismogenetic system. The degree of correlation is generally higher in the southern SAF segment, which is consistent with the observation of shorter return periods for large earthquakes. A plausible explanation is that because aftershock sequences are localized in space and time, their efficient removal unveils long-range background interactions which are obscured by their presence! Our results indicate complexity in the expression of background seismicity along the San Andreas Fault, with criticality being a very likely mechanism as a consequence of the persistent non-equilibrium inferred from the temporal entropic index. However, definite conclusions cannot be drawn until the earthquake record is exhaustively studied in all its forms.

Key words: Tsallis entropy, complexity, non-extensivity, San Andreas Fault, seismicity.

1. Introduction

Seismicity is generally thought to comprise a mixture of a background process that expresses the continuum of tectonic deformation in a given seismogenetic area and a population of aftershock sequences (foreground process) that express the short-term activity associated with significant background events. The statistical physics of background seismicity, hence the nature of the seismogenetic system, is not clear. In consequence, the way in which seismicity and tectonic deformation evolve is also not well understood, with significant repercussions on problems such as hazard analysis and long-term forecasting.

There are two principal approaches towards understanding the statistical physics of seismicity. The first and currently most influential) postulates that the expression of the background process is Poissonian in time and space and obeys *extensive* Boltzmann-Gibbs thermodynamics. It is important to emphasize that this property is associated only with the time and the distance (space) between earthquake events, but not with their size (magnitude) which is governed by the well-established frequency – magnitude (F-M) relationship of Gutenberg and Richter[1]. Paradigmatic expression of this viewpoint is the Episodic Type Aftershock Sequence (ETAS) (e.g. Ogata, 1988, 1998; Zhuang et al, 2002; Helmstetter and Sornette, 2003; Touati et al, 2009; Segou et al, 2013). In this empirical construct which essentially expresses a self-excited conditional Poisson process (Hawkes, 1972; Hawkes and Adamopoulos, 1973; Hawkes and Oakes, 1974), the randomly occurring background main events trigger their aftershock sequences in which aftershocks trigger their own sub-sequences thus leading to short-term clustering of multiple generations of foreground events; these are dependent on each other and their time dependence is described by a power law known as the Omori-Utsu law of aftershocks (e.g. Utsu et al., 1995). There are also point process models developed to address the problem of intermediate to long-term clustering, as for instance the EEPAS (Each Earthquake is a Precursor According to Scale, e.g. Rhoades, 2007) and the PPE (Proximity to Past Earthquakes, e.g. Marzocchi and Lombardi, 2008). In any case, point processes are memoryless, therefore at the core of this viewpoint rests the assumption that background earthquakes are statistically independent and although it is possible for one event to trigger another (smaller or larger), this occurs in an unstructured random fashion and does not to contribute to the long-term evolution of seismicity.

The second viewpoint postulates that the seismogenetic process comprises a complex system, although the mechanisms begetting complexity are not clear as yet. A well-studied class of models (Bak and Tang, 1989; Sornette and Sornette, 1989; Olami et al., 1992; Sornette and Sammis, 1995; Rundle et al., 2000; Bak et al, 2002; Bakar and Tirnakli, 2009; many others) suggests that seismicity expresses a non-equilibrating fractal tectonic grain that continuously evolves toward a stationary critical condition with no characteristic spatiotemporal scale (Self Organized Criticality - SOC). In this

[1] An apparent contradiction is that the scale-free grading between earthquake frequency and magnitude implied

view, all earthquakes belong to, or evolve towards the same global population and participate in shaping a non-equilibrium state in which events develop spontaneously and any small instability has a chance of cascading into a large shock. Critical complex systems evolving in a fractal-like space-time are characterized by long-range interactions and long-term memory which, at least at a regional scale, should be manifested by correlations and power-law distributions observable in the statistical behaviour of their energy release, temporal dependence and spatial dependence. In addition, there are models proposing alternative complexity mechanisms that do not involve criticality, yet maintain the seismogenetic system in a state of non-equilibrium (see Sornette and Werner, 2009 for a discussion). More recently, the Coherent Noise Model (Newman, 1996) was applied to seismicity by Celikoglu et al, (2010). This is based on the notion of external stress acting coherently onto all agents of the system without having any direct interaction with them and is shown to generate power-law interevent time distributions. A weak point in this model is that it does not include some geometric configuration of the agents and it is not known how this would influence the behaviour of the system.

A fundamental difference between the Poissonian models and SOC is their understanding of the background seismogenetic process. The former approach assumes a self-exciting Poisson process in time and space, in which there is no correlation (interaction) between background events, so that the statistical description of parameters pertaining to their temporal and spatial evolution would be consistent with the Boltzmann-Gibbs formalism. The SOC formalism requires short and long-range interactions in a non-equilibrium state, so that there would be *correlation* between background events, as well as between background/foreground events and foreground/foreground events. This renders memory to the system and the statistics of the parameters pertaining to its temporal and spatial evolution are expected to exhibit power-law behaviour and long tails. Moreover, non-critical complexity models cannot develop power-law distributions in space and time, unless they evolve in non-equilibrium states. Poissonian models and SOC both agree that the foreground process (aftershock sequences) comprise a set of dependent events, but whereas the former assign only local significance to this dependence, SOC considers them to be an integral part of the regional seismogenetic process.

The above discussion makes clear that were it possible to identify and remove the foreground process (aftershocks), it might also be possible to clarify the nature and dynamics of the background process by examining its spatiotemporal characteristics for the existence of correlation (hence non-extensivity). This is not a simple objective and before it is pursued, there must be satisfactory answers to three basic requirements, which are: (a) Statistical physics that comprise a *natural* and befitting (*not* model-based) general context in which to investigate the existence of correlation; (b) Appropriate parameters for the analysis of correlation in the temporal and spatial properties of seismicity and, (c) Effective ways of distinguishing the background from the foreground processes. It turns out that satisfactory (or nearly satisfactory) answers exist, as will be elaborated forthwith.

---

by the F-M relationship cannot be derived from the Boltzmann-Gibbs formalism.

The most recent development in the statistical description of earthquake occurrence is the introduction of Non Extensive Statistical Physics (NESP) as a fundamental conceptual framework of the thermodynamics that govern seismogenesis and seismicity. NESP has been developed by Tsallis (1988, 2009) as a generalization of the (extensive) Boltzmann-Gibbs formalism to non-extensive (non-equilibrating) systems. As such it comprises an appropriate tool for the analysis of complexity evolving in a fractal-like space-time and exhibiting scale invariance, long-range interactions and long-term memory (e.g. Gell'mann and Tsallis, 2004). NESP predicts power-law cumulative probability distributions for non-extensive (complex) dynamic systems, which reduce to the exponential cumulative distribution in the limiting case of extensive (random) systems. Thus, NESP provides a unique, consistent and *model-independent* theoretical context in which to investigate the nature and dynamics of the background and foreground seismogenetic processes.

With respect to the second requirement above, a common measure of scaling in earthquake size is the Gutenberg – Richter F-M distribution, which is interpreted to express the scale-free statistics of a fractal active tectonic grain. The F-M distribution is *static* and does not say much about the temporal dynamics (evolution) and spatial dynamics of the seismogenetic system. It also says nothing about correlation in the characteristics of energy release, since it does not relate the energy released by a given earthquake to the energy released by its predecessor or successor events. Nevertheless, this undisputable empirical relationship is a yardstick against which to compare any physical and statistical description of the relationship between earthquake size and frequency and as such will be used herein.

A measure of the temporal dynamics and definite measure of possible correlation between successive earthquakes is the time elapsed between consecutive events above a magnitude threshold over a given area: this parameter is variably referred to as *interevent time, waiting time, calm time* etc. Understanding the statistics of the earthquake frequency – interevent time (F-T) distribution is obviously of paramount importance for understanding the dynamics of seismogenetic system and have been studied by several researchers, albeit not as extensively as its F-M counterpart. The empirical F-T distributions generally exhibit power-law behaviour and long tails. In the context of Extensive Statistical Physics, they have been investigated with different standard statistical models with tails, reducible to power laws in some way or another; examples of this approach are the gamma distribution and the Weibull distribution (e.g. Bak et al., 2002; Davidsen and Gold, 2004; Corral, 2004; Martinez et al, 2005; Talbi and Yamazaki, 2010). Corral (2004) has applied the gamma distribution and has suggested universality analogous to the Gutenberg – Richter F-M distribution, to which other investigators objected on the basis of self-exciting conditional Poisson models and suggested that the interevent times are mixed distributions of correlated aftershock and uncorrelated background processes (e.g. Saichev and Sornette, 2013; Hainzl et al, 2006; Touati et al, 2009). Interestingly enough, Molchan (2005) has shown that for a stationary point process, if there is a universal

distribution of interevent times, then it must be exponential! The few investigations performed in the context of Non Extensive Statistical Physics will be reviewed in Section 2.2. It should be emphasized that hitherto studies have analysed the mixed background/foreground processes and have not focused on the background process independently.

With respect to the third requirement, (discrimination of background and foreground processes), we have chosen to implement the state-of-the-art stochastic declustering method of Zhuang et al (2002). As will be elaborated in Section 3, this has an additional for our purposes "advantage", in that it comprises a *paradigmatic* realization of the self-excited Poisson process. Accordingly, if the background seismicity obeys Boltzman-Gibbs statistics, then this method should be able to extract a nearly random background process against which to test the alternative hypotheses (NESP). If it is does not, then the argument in favour of a complex background process is stronger.

The present study is part of a systematic attempt to examine the dynamics of the seismogenetic system by implementing the generalized NESP formalism and searching for signs of randomness or self-organization as a function of time. The remaining of this presentation is organized as follows. A brief exposé of the NESP formalism will be given in Section 2.1, followed by a presentation of its implementation to the analysis of *joint* frequency – magnitude – interevent time (F-M-T)(Section 2.2). The analysis will focus on seismicity along the San Andreas Fault, California, U.S., because it is a very well-studied area with very reliable earthquake monitoring services and seismological catalogues. A brief presentation of the geotectonic context and a thorough presentation of the data (earthquake catalogues) and the data reduction and analysis procedures will be given in Section 3. Section 4 is devoted to the presentation of the results and of the validation tests conducted in order to appraise their rigour. Finally, it shall be demonstrated that the frequency of earthquake occurrence along the San Andreas Fault is multiply related to the magnitude and the interevent time by well-defined bivariate power-laws consistent with NESP and that the seismicity is generated by an apparently complex system comprising a mixture of correlated background and correlated foreground processes.

2. Non-Extensive Statistical Physics

2.1 Tsallis entropy and probability distribution

Let X be a seismicity parameter (e.g. energy, interevent time etc.) and $p(X)dX$ the probability of finding its value in $[X, X+dX]$ so that $\int_W p(X)dX = 1$, where W is the support of X and expresses the total number of microscopic configurations of the seismogenetic system. Non-equilibrium states in systems with complex behaviour can be described by the Tsallis (1988) entropic functional:

$$S_q = k\frac{1}{q-1}\left[1-\int_W p^q(X)dX\right], \quad (1)$$

where k is the Boltzmann constant and q the *entropic index* which is a measure of the *non-extensivity* of the system. For the particular case q = 1 Eq. 1 reduces to the Boltzmann–Gibbs (BG) entropy

$$S_{BG} = -k\int_W p(X)\ln(p(X))dX$$

The Tsallis entropy shares properties with the BG entropy including concavity and the fulfilment of the H-theorem. However, it is *pseudo-additive* ($q \neq 1$) in the sense that unlike the S_{BG}, it is generally not proportional to the number of the elements of the system. This leads to *super-additivity* if q<1, *additivity* when q=1, (that is Gibbs-Boltzmann statistics), and *sub-additivity* if q>1.

The maximization of the Tsallis entropy yields the *q-exponential distribution:*

$$p(X) = \frac{1}{Z_q}\exp_q\left[-\frac{\lambda}{I_q}\left(X-\langle X\rangle_q\right)\right], \quad (2)$$

where $\langle X\rangle_q = \int_W Xp_q(X)dX$ is the *q-expectation* value of X, λ is an appropriate Lagrange multiplier, $Z_q = \int_W dX \exp_q\left[-\lambda\cdot I_q^{-1}\cdot\left(X-\langle X\rangle_q\right)\right]$ is a generalized canonical partitioning function and $I_q = \int_W dX[p(X)]^q$. In Eq. 2, $\exp_q(.)$ represents the *q-exponential* function

$$\exp_q(X) = \begin{cases}\left(1+(1-q)X\right)^{\frac{1}{1-q}} & 1+(1-q)X>0\\ 0 & 1+(1-q)X\le 0\end{cases}, \quad (3)$$

which comprises a generalization of the exponential function: for q=1, $\exp_q(X) = e^x$. As evident from Eq. (2) and Eq. (3), the probability $p(X)$ is a power-law with a long tail if q>1, corresponding to *sub-additivity*, an exponential distribution if q=1, corresponding to *additivity*, and a *cut-off* if 0< q< 1, corresponding to *super-additivity*; the cut-off appears at $X_c = X_0(1\text{-}q)^{-1}$, with $X_0 = (1\text{-}q)\cdot\langle X_q\rangle + \lambda/I_q$.

If the *empirical* distribution of X (i.e. the *escort probability*) is $P_q(X)$, then the *cumulative* probability function (CDF) derived from the above analysis is:

$$P(>X) = \int_X^\infty dX\ P_q(X).$$

For q > 1 and $X \in [0, \infty)$, the CDF becomes:

$$P(>X) = \int_X^\infty dX\ P_q(X)\ldots\Rightarrow\ldots P(>X) = \exp_q\left(-\frac{X}{X_0}\right) = \left[1-(1-q)\left(\frac{X}{X_0}\right)\right]^{\frac{1}{1-q}} \quad (4)$$

which is a *q-exponential distribution.*

Figure 1 illustrates the q-exponential CDF for different values of q. When q > 1 the CDF exhibits a tail that becomes longer with increasing q; the system experiences long-range correlation and has long-term memory. When q = 1, the q-exponential distribution reduces to the common exponential

distribution: the system is a random process (uncorrelated and memoryless). When $q < 1$, the distribution exhibits a cut-off, i.e. P (>X) = 0 and is characterized by a bounded correlation radius whenever the argument becomes negative.

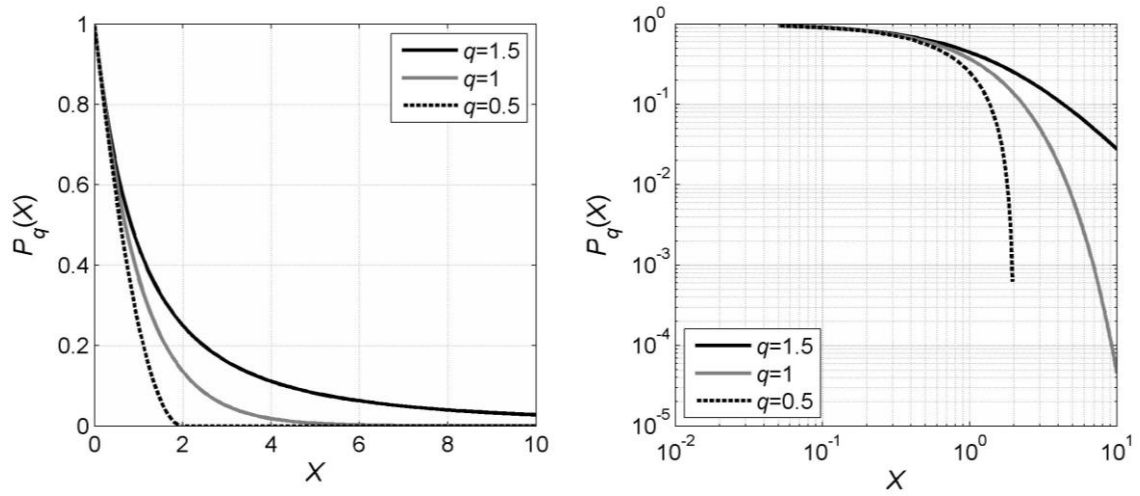

Figure 1. Examples of the *q*-exponential CDF for different values of *q*, plotted in linear scale (left) and double-logarithmic scale (right).

2.2 NESP aprroach to earthquake statistics

The Non-Extensive Statistical Physics (NESP) approach has attracted growing attention during the past few years (e.g. Vallianatos and Telesca, 2012) with several researchers studying the properties of the F-M and F-T distributions (see below). A number of NESP compatible models have been proposed for the frequency-magnitude distributions (Sotolongo-Costa and Posadas, 2004; Silva et al., 2006; Telesca 2011, 2012 etc.). These all consider the composite interaction of two rough fault walls (asperities) and the rock fragments filling the space between them (fragment-asperity model). This interaction is supposed to modulate earthquake triggering. However, the three models differ in their assumption of how the total energy stored in the asperities and fragments scales with their linear characteristic dimension. Herein, we postulate that the assumption made by Telesca (2011, 2012), that the energy scales with the area of the fragments and asperities ($E \propto r^2$) so that $M = \frac{2}{3}\log(E)$, is representative of the seismogenetic process as it is compatible with the well-studied rate-and-state friction laws of rock failure. Accordingly, we adopt this model, in which the cumulative frequency-magnitude distribution reads:

$$P(>M) = \frac{N(>M)}{N_0} = \left(1 - \frac{1-q_M}{2-q_M} \cdot \frac{10^M}{\alpha^{2/3}}\right)^{\left(\frac{2-q_M}{1-q_M}\right)}. \quad (5)$$

In Eq. (5), N is the number of earthquakes with magnitude greater than a threshold M, N_0, is the total number of earthquakes at $M = 0$, α is a constant that expresses the proportionality between the

released energy E and the fragment size r and q_M is the relevant entropic index.

The application of NESP to the analysis of one-dimensional F-T distributions has been attempted by only a handful of authors, exclusively on the basis of and the CDF expressed by Eq. (4). The emergence of q-exponential distributions in critical seismicity models was investigated by Caruso et al (2007) and Bakar and Tirnakli (2009), while the same for non-critical models was investigated by Celikoglu et al (2010). Vallianatos et al. (2012) observed non-extensive spatiotemporal behaviour during tri-axial deformation of rock samples. In a series of empirical studies, Abe and Suzuki (2005) analysed the temporal properties of the seismicity in California and Japan and Carbone et al (2005) in Italy. More recently, Vallianatos et al. (2012) investigated the spatiotemporal properties of the 1996 Aigion (Greece) aftershock sequence, Vallianatos et al. (2013) the temporal behaviour of the 2011-2012 seismicity crisis in the Santorini volcanic complex (Greece) and Vallianatos and Sammonds (2013) the behaviour of global seismicity prior to the 2004 Sumatran and 2011 Honsu mega-earthquakes. Additional strong evidence of non-extensive spatiotemporal behaviour in Greek seismicity has been presented by Papadakis et al (2013) and Michas et al (2013). In the empirical studies, the F-T distributions $P(>T)$ were effectively fitted with a one-dimensional q-exponential.

In taking this line of research a step forward, we note that it is also possible to construct multivariate frequency distributions that express the *joint* probability of observing an earthquake above a given magnitude *and* a given interevent time and/or interevent distance. For example, a joint frequency – magnitude – interevent time (F-M-T) distribution can be constructed thus: A threshold (cut-off) magnitude M_{th} is set and a bivariate frequency table (histogram) H, representing the *incremental distribution*, is first compiled. The cumulative distribution is obtained from the incremental distribution by backward bivariate summation, according to the scheme

$$N_{m\tau} = \sum_{j=D_\tau}^{\tau} \sum_{i=D_M}^{m} H_{ij}, \quad \tau = 1,\ldots D_T, \quad m = 1,\ldots D_M$$
$$N_{m\tau} \neq 0 \quad \Leftrightarrow \quad H_{m\tau} \neq 0$$

where , D_M is the dimension of H along the magnitude axis and D_T is the dimension of H along the T axis. The (posterior) constraint on $N_{m\tau}$ ensures that the locations of the unpopulated bins will not be replaced by a carpet of outliers. In this construct, the cumulative frequency (earthquake count) can be written thus: $N(\{M \geq M_{th}, T : M \geq M_{th}\})$. Then, the empirical probability $P(>\{M \geq M_{th}, T : M \geq M_{th}\})$ is simply

$$\frac{N\left(>\{M \geq M_{th}, T : M \geq M_{th}\}\right)}{N_0}. \qquad (6)$$

By assuming that the magnitude (M) and interevent time (T) are statistically independent so that the joint probability $P(M \cup T)$ factorizes into the probabilities of M and T in the sense $P(M \cup T) = P(M)P(T)$, the joint probability $P(>\{M > M_{th}, T : M > M_{cth}\})$ can be expressed as

$$\frac{N\left(>\{M \geq M_{th},\ T : M \geq M_{th}\}\right)}{N_0} = \left(1-\frac{1-q_M}{2-q_M}\cdot\frac{10^M}{\alpha^{2/3}}\right)^{\left(\frac{2-q_M}{1-q_M}\right)}\cdot\left(1-(1-q_T)\cdot\frac{T}{T_0}\right)^{\frac{1}{1-q_T}}, \quad (7)$$

where q_M and q_T are the entropic indices for the magnitude and interevent times respectively and T_0, is the *q-relaxation time*, analogous to the relaxation (characteristic) time often encountered in the analysis of physical systems. On taking the logarithm and setting a = log(N_0), and $c = T_0^{-1}$, Eq. (7) becomes

$$\log N\left(>\{M \geq M_{th},\ T : M \geq M_{th}\}\right) = \\ = a \quad + \quad \left(\frac{2-q_M}{1-q_M}\right)\cdot\log\left(1-\frac{1-q_M}{2-q_M}\cdot\frac{10^M}{\alpha^{2/3}}\right) \quad + \quad \frac{1}{1-q_T}\log\left(1-c(1-q_T)T\right) \quad (8)$$

Eq. 8 is a generalized (bivariate) law of the Gutenberg – Richter kind in which

$$b_q = \frac{(2-q_M)}{(q_M-1)} \quad (9)$$

is the NESP equivalent of the *b* value (e.g. Telesca, 2012). Accordingly, Eq. (8) is the general model to be implemented in the ensuing analysis.

If the seismogenetic process is non-extensive (earthquakes occur in correlated space-time), then:

- b_q should be equivalent to the *b* value computed by conventional methods because the distribution of magnitudes does not relate the energy released by a given earthquake to the energy released by its successor events, but only conveys information about the geometry of the active fault system.
- q_T should differ from unity, thus expressing the interdependence of successive events in the correlated space-time of the seismogenetic system.

On the other hand, if earthquakes appear spontaneously in a self-excited random system, b_q should still be equivalent to the *b* value computed by conventional methods but $q_T \to 1$ and the third term in the RHS of Eq. (7) should reduce to the logarithm of the exponential distribution. In both cases, the favourable comparison of b_q (that is q_M) to the results of well-established methods of *b* value estimation should be a rather robust means of ensuring the validity of the numerical procedure used in approximating Eq. (8) and the robustness of the results and conclusions.

3. Earthquake data and analysis procedures

As stated in the introduction, our presentation will focus on the analysis of seismicity along the San Andreas Fault, California, U.S., because it is a very well-studied area, with very reliable earthquake monitoring services and seismological catalogues. Moreover, Californian seismicity is practically the test bed for the development of seismogenetic models; therefore, it is an appropriate place to begin our investigations. The SAF system (main and "sibling" faults) is generally taken to comprise three major

segments: The southern (Mojave) segment begins near the Salton Sea at the SE corner of California (approx. 33.36°N, 115.7°W) and runs up to Parkfield, Monterey County (approx. 35.9°N, 120.4°W); the central segment extending between Parkfield and Hollister (approx. 36.85°N, 121.4°W) and the northern segment extending from Hollister through the San Francisco bay area to the Mendocino Triple Junction (approx. 40.36°N, 124.6°W). The geographic boundaries between these segments are not clearly defined. While the overall motion on the SAF is right-lateral strike-slip, there are local variations in the mode of deformation along the strike of the fault (e.g. Jones, 1988; Hardebeck and Hauksson, 2001). The most important of those is the so-called "Big Bend", located approx. between 37.7°N and 35.1°N, where the SAF intersects with the major left-lateral strike-slip Garlock fault and forms a restraining bend. Studies based on slip rates, focal mechanisms etc. indicate that this is the area where the SAF locks up in Southern California and a tectonic boundary forms between the north and central SAF segment on one hand, and the south SAF segment on the other (e.g. Fialko, 2006; Becker et al, 2005). Accordingly, and for the purposes of this presentation, we divide and study the seismicity of the SAF in two parts, as shown in Fig. 2: the *northern SAF* between Parkfield and the Mendocino Triple Junction, (henceforth referred to as nSAF), and the *southern SAF* between Salton Sea and the Garlock fault (henceforth referred to as sSAF).

The areas of Mendocino Triple Junction and Garlock Fault are not included in the present analysis which focuses exclusively on domains experiencing pure right-lateral strike-slip deformation. We consider that the expression of seismicity in the above two areas has to be studied separately as they both represent significant geodynamic features whose seismicity is not exclusively associated with the SAF. The Mendocino Fracture Zone includes the most seismically active part of the California (Yeats, 2013) and according to Dengler et al (1995) the north coastal region accounted for about 25% of the seismic energy released in California in a 50 year period. The Mojave segment – Garlock fault area is characterized by a mixture of reverse and strike slip faulting mechanisms, while the Garlock Fault is a major boundary between the semi-rigid microplate of Basin and Range Province and the Mojave Desert and is believed to have developed in order to accommodate the strain differential between the extensional tectonics of the Great Basin crust and the right lateral strike-slip faulting of the Mojave Desert crust.

The earthquake data utilized in this study was extracted from the regional earthquake catalogues of the North California Seismic Network (NCEDC @ http://www.ncedc.org) and South California Earthquake Data Centre (SCEDC @ http://www.data.scec.org). The former (NCEDC catalogue) comprises 16,743 events recorded between 1969 and 2012 in the area 42ºN – 36ºN and -126ºE – -114ºE. The latter (SCEDC catalogue) comprises 28,882 events recorded between 1980 and 2012 in the area 36ºN – 32ºN and -126ºE – -114ºE. In both catalogues, most earthquakes are reported in the M_L and M_w magnitude scales while there is a considerable number of events in the duration (M_d) and amplitude (M_x) scales. The latter have been exhaustively calibrated against the M_L scale: Eaton (1992)

has shown that they are *within* 5% of the M_L scale for magnitudes in the range 0.5 to 5.5 and that they are virtually independent of the distance from the epicentre to at least 800 km. In consequence, M_d and M_x are practically equivalent to M_L. For the purpose of the present analysis the M_w magnitudes were also converted to M_L using the empirical formula of Uhrhammer et al (1996): $M_w = M_L \cdot (0.997 \pm 0.020) - (0.050 \pm 0.131)$. Thus, both NCEDC and SCEDC catalogues have been reduced to the M_L scale and are homogenous and complete for $M_L \geq 3.1$ and $M_L \geq 2.5$ respectively, for the period 1980-2011. Fig. 2 illustrates the epicentre distribution of a merged version of the two catalogues, in which duplicate events have been removed. Fig. 3-left and 3-right illustrate the corresponding cumulative earthquake counts (solid black lines).

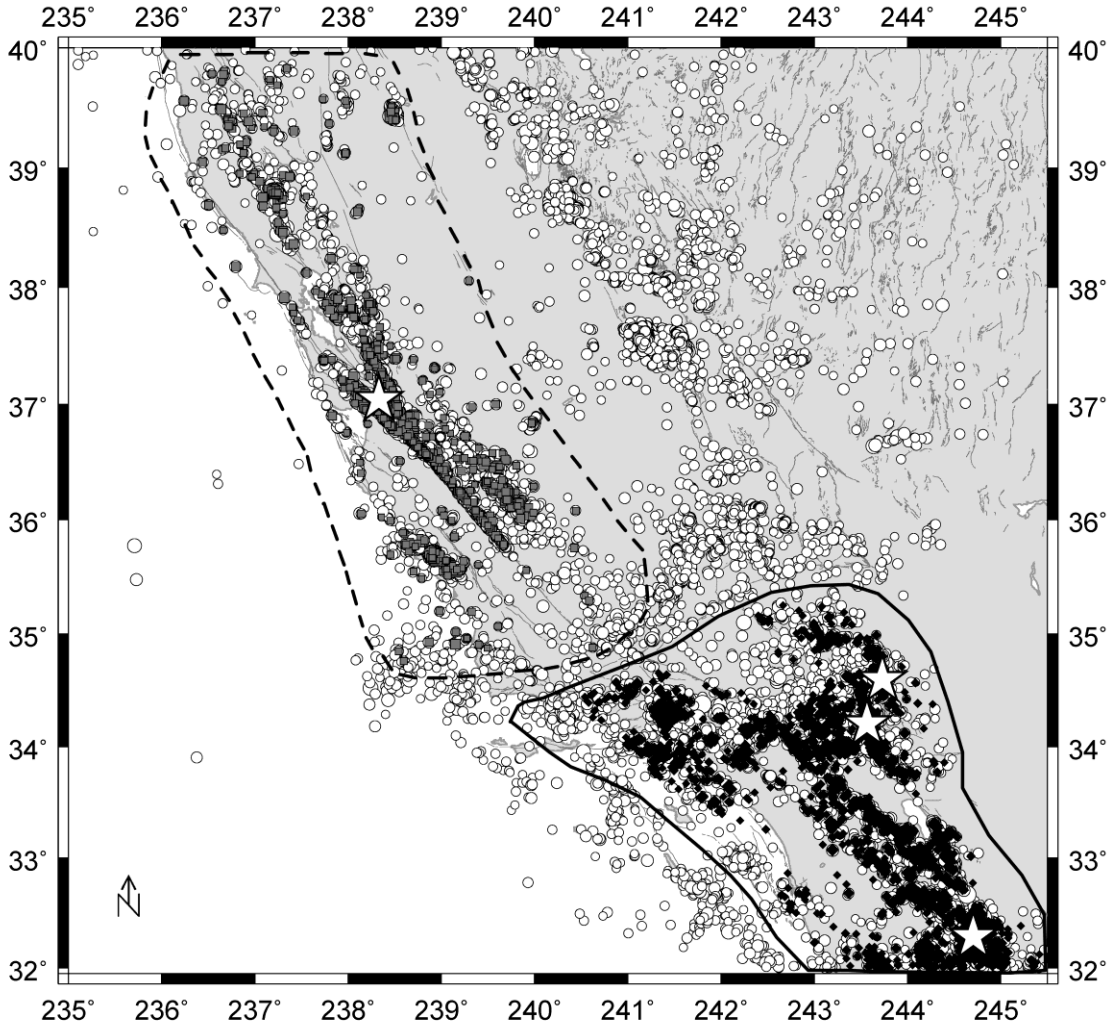

Figure 2. Epicentral maps of the raw and declustered earthquake catalogues used herein. The white circles represent the epicentres of the merged and homogenized NCEDC and SCEDC raw catalogues. The dashed polygonal line outlines the northern stretch of the SAF and its associated seismicity (nSAF). The grey squares represent the epicentres of the declustered nSAF catalogue (1196 events with probability ≥ 70% to be background). The solid polygonal line encloses the southern stretch of the SAF segment and its associated seismicity (sSAF). The black diamonds represent the epicentres of the declustered sSAF catalogue (3200 events with probability ≥ 70% to be background). The white stars indicate the epicentres of the major Loma Prieta, Landers, Hector Mine and Baja earthquakes.

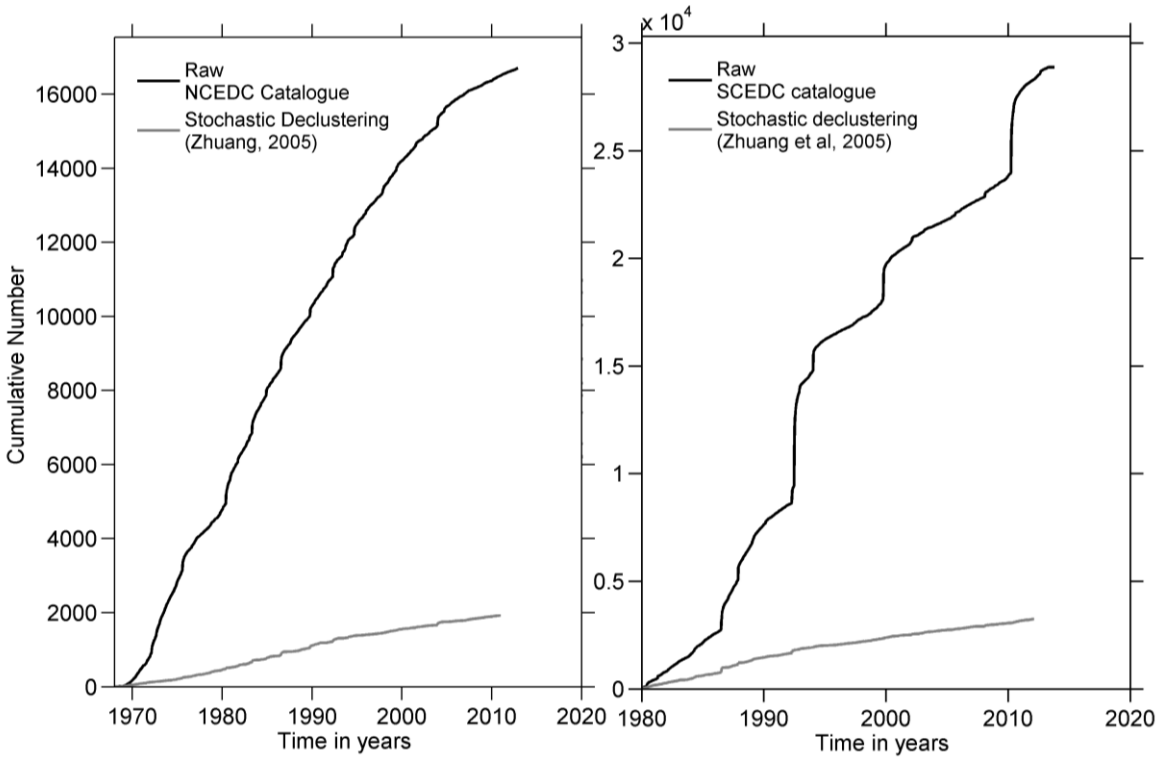

Figure 3. Left: The cumulative earthquake count of the observed (raw) and declustered NCEDC catalogues are illustrated with the black and grey solid lines respectively. **Right:** Same for the raw and declustered SCEDC catalogues.

Fig. 4a and Fig. 4b illustrate a typical example of the empirical F-M-T distribution compiled from the *raw* NCEDC catalogue for $M_c \geq 3.4$ (5,067 events). It is an apparently well defined and structured surface, with one end-member at $[M \geq M_c, T=0]$ comprising the one-dimensional Gutenberg – Richter law and the other end-member at $[M_c = 0, T]$ comprising the one-dimensional F-T distribution. The logarithmic form of the distribution is shown in Fig. 4b and has been approximated with the model of Eq. (8) using non-linear least-squares solver. Because all the parameters of Eq. (8) are subject to positivity constraints and the entropic indices are also bounded, a solver implementing the trust-region reflective algorithm was chosen (e.g. Moré and Sorensen, 1983; Steihaug, 1983), together with *Least Absolute Residual minimization* so as to down-weight possible outliers. A typical outcome of this procedure is shown in Figs. 4c and 4d. The quality of the approximation is exceptional and the correlation coefficient (R^2) is as high as 0.99. The magnitude entropic index q_M is 1.5 so that $b_q \approx 1$. The temporal entropic index q_T is 1.30 indicating weak non-extensivity. The evaluation of the result is summarized in Fig. 4d and is based on the analysis of the statistical distribution of the residuals. Thus, the observed cumulative probability of the sorted residuals is numerically approximated with a normal location-scale distribution (dashed line) and a Student-t location-scale distribution (solid line). Evidently, the residuals are not normally distributed and exhibit tails that are better approximated with the *t*-location-scale distribution. However, only 25 residuals deviate from the normal distribution, out of 173, or 14.45%; these represent outliers that have been effectively suppressed, since the solution is determined by the remaining 85.5% of the observations. It can also be seen that only 8 residuals are

greater than |0.5|, representing 3.16 earthquakes; these are, more or less scattered at the tails of the observed F-M-T distribution.

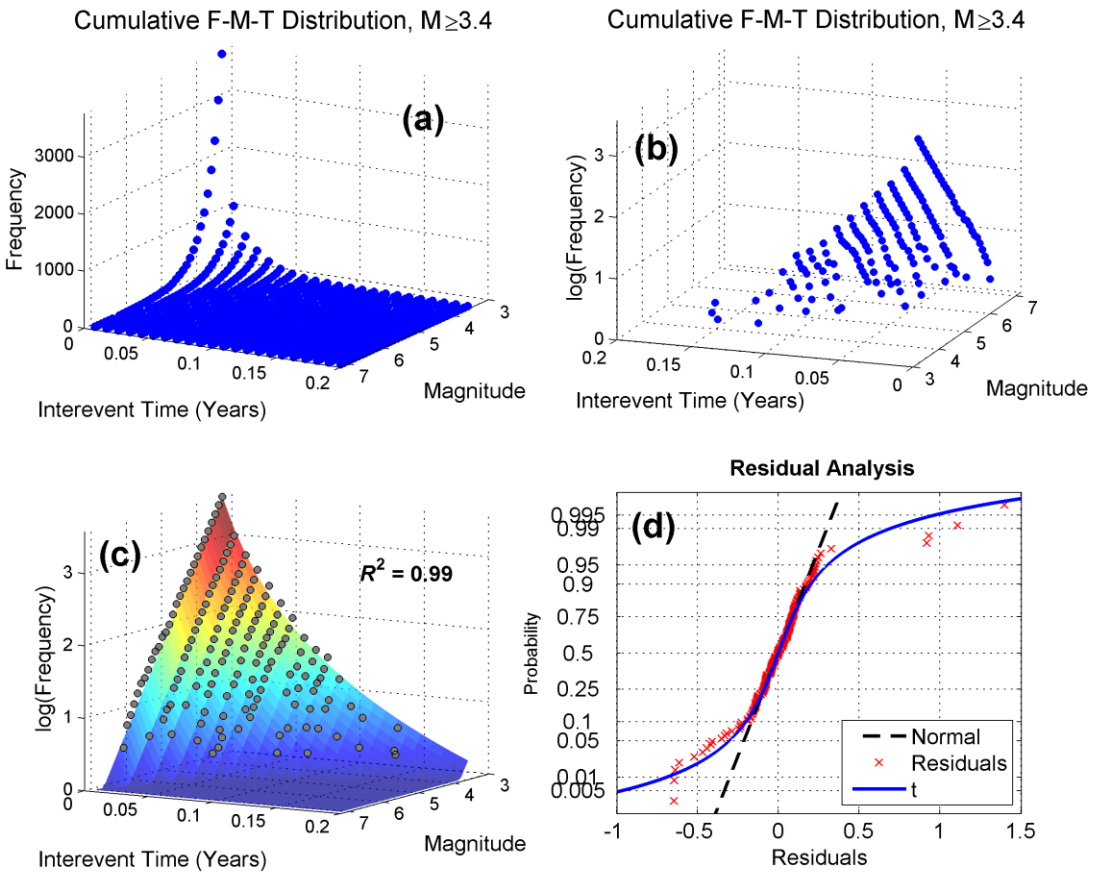

Figure 4. (a) is the F-M-T distribution for the entire raw NCEDC catalogue and a threshold magnitude $M_{th} \geq 3.4$ (5067 events); **(b)** the same F-M-T but in logarithmic frequency scale and viewed from the opposite direction; **(c)** as per **(b)** but shown with the model fitted using Eq. (8); **(d)** is a probability analysis of the residuals (see Section 3 for details).

3.1 Declustering

As stated in the introduction, it is not at all clear whether the background seismogenetic process is fundamentally random or correlated, let alone that there has been a (very relevant) debate as to whether the power laws implied by the empirical F – T distributions are characteristic and universal, or only a result of mixing correlated foreground and uncorrelated background processes. In order to address these questions with the formalism expressed by Eq. (8) and determine entropic indices appropriate for the mixed and background processes, it is imperative to conduct the analysis on *declustered* versions of the NCEDC and SCEDC catalogues, in which the aftershock sequences have been eliminated in an optimal as possible way.

Methods to separate the background and foreground processes (*declustering*) have evolved from deterministic, which classify each earthquake as a main shock or aftershock, to stochastic, which assign each earthquake with a probability that it is an aftershock of each preceding earthquake. An excellent review is provided by van Stiphout et al, (2012). The principal examples of deterministic methods are those by Gardner and Knopoff (1974) and Reasenberg (1985). The former identifies aftershocks using inter-event distances in time and space (windows), usually as function of the main shock magnitude. It also ignores higher order aftershocks, i.e. aftershocks of aftershocks. The latter allows for aftershock triggering within a cluster and uses Omori's law as a measure of the temporal dependence of aftershock activity. Both methods ignore fault elongation for larger magnitude events, assuming circular (isotropic) spatial windows. Stochastic declustering has been pioneered by Zhuang et al. (2002) and is based on space-time branching approaches to describe how each event triggers its successors. This generalizes and improves on the previous methods because the choice of the space-time distance is optimized by fitting an ETAS model to the earthquake data and there is no need to assume anything about the parameters pertaining to the definition of the space-time distance (although a parametric form of said distance is assumed a priori). More significantly, however, instead of associating an aftershock to only one main shock, the method assigns each earthquake with a probability that it is an aftershock of each preceding earthquake, meaning that all preceding earthquakes are possible main shocks of the events that follow them. This is advantageous in that it circumnavigates the difficulty of making committing binary decisions in the (very frequent) case of nearly equal space-time distances between successive events. The use of the ETAS model may be a limitation, as it imposes the parametric form of the space-time distance. Marsan and Lengliné (2008) have carried stochastic declustering a step forward by introducing a generalized triggering process without a specific underlying model, although in this approach as well background earthquakes are assumed to occur at constant and spatially uniform rate density. Herein we implement the stochastic declustering method of Zhuang et al (2002), the principal reason being that it based on the *paradigmatic* realization of the self-excited Poisson process: if background seismicity obeys Boltzman-Gibbs statistics, then this method should be able to extract a nearly random background process against which to test the alternative hypotheses.

The Zhuang et al method uses the following form of the normalized probability that one event will occur in the next instant, conditional on the hitherto history of the seismogenetic process (conditional intensity):

$$\lambda(t,x,y,M \mid H_t) = \mu(x,y,M) + \sum_{i:t_i<t} \kappa(M_i)\cdot g(t-t_i)\cdot f(x-x_i, y-y_i \mid M_i)\cdot j(M \mid M_i) \qquad (10)$$

In Eq. 10, λ is the conditional intensity on the history of observation H_t until time t, $\mu(x,y,M)$ is the background intensity, $\kappa(M)$ is the expected number of foreground events triggered by a magnitude M main shock and $g(t)$, $f(x,y|M_i)$ and $j(M|M_i)$ are respectively the probability distributions of the

occurrence time, the location and the magnitude events triggered by a main shock of magnitude M_i. If the catalogue is arranged in chronological order, then the probability of an event j to have been triggered by an event $i < j$ can be estimated from the occurrence rate at its occurrence time and location as

$$p_{i,j} \frac{\kappa(M_i) \cdot g(t_j - t_i) \cdot f(x_j - x_i, y_j - y_i \mid M_i)}{\lambda(t_j, x_j, y_j \mid H_t)}$$

and the probability that an event j is aftershock is given by

$$p_j = \sum_{i=1}^{j-1} p_{i,j}$$

Conversely, the probability that an event j is background is given by

$$\phi_j = 1 - p_j = \frac{\mu(x_j, y_j \mid H_t)}{\lambda(t_j, x_j, y_j \mid H_t)}$$

The algorithm runs iteratively through the catalogue and by assigning probabilities $p_{i,j}$, p_j and ϕ_j to the j^{th} event generates the foreground sub-process associated with the i^{th} event (i.e. its aftershock sequence). It thus separates the catalogue into a number of sub-processes whose initiating events comprise the background.

As a rule of thumb, an event with $\phi_j \leq 50\%$ is taken to be foreground while an event with $\phi_j > 50\%$ is likely to belong to the background. Since the output of stochastic declustering is not unique, it is useful to use the probabilities $p_{i,j}$ and ϕ_j to generate different realizations of the declustered catalogue at different probability levels and use them to test hypotheses associated with background seismicity and/or aftershock clustering. In this initial and exploratory presentation, we will not go into such detail. Rather, we assume that events with probability $\phi_j > 70\%$ belong to the background. Accordingly, the declustered NCEDC and SCEDC catalogues consist of 1,920 and 3,225 events respectively and are complete for $M_L \geq 3.1$ and $M_L \geq 2.5$ respectively for the period 1980-2011. Their associated cumulative earthquake counts are illustrated in Fig. 3a and Fig. 3b respectively (solid grey lines); they are almost free of the time-local rate changes (jerks) evident in the corresponding cumulative counts of the raw catalogues due to the inclusion of aftershocks. Nevertheless, they are not completely smooth and exhibit small fluctuations because at the 70% probability level, some residual foreground events are still present in the declustered catalogues. In response, we also seek to confirm the results obtained at the 70% level by studying a subset of 1,724 the SCDEC events with probability $\phi_j > 90\%$ to be background; the outcome of this experiment is presented as part of the Discussion in Section 5.

In the ensuing analysis we shall use subsets of the raw and declustered NCEDC and SCEDC catalogues, directly associated with the nSAF and sSAF segments as indicated in Fig. 2; these are

henceforth to be referred to as the nSAF and sSAF catalogues. The raw nSAF catalogue comprises 7912 events; the declustered nSAF catalogue comprises 1196 events, indicated with grey squares in Fig. 2. Respectively, the raw sSAF catalogue comprises 26306 events and the declustered sSAF catalogue 3200 events indicated with black diamonds.

4. Results

4.1 Entropic indices

As repeatedly stated above, we seek to investigate the nature of the seismogenetic process along the SAF and study its time dependence, with particular reference to periods preceding large ($M_L > 7$) earthquakes. To do this we compile F-M-T distributions over consecutive overlapping windows and solve them for the parameters a, α, q_M, c and q_T of Eq. (8). The procedure is applied to the raw and declustered nSAF and sSAF catalogues, starting at year 1980 and ending at year 2012. The F-M-T distributions are formed in the natural time of the respective seismogenetic processes: for the raw and declustered nSAF catalogues, each window comprises 450 consecutive events; for the raw and declustered sSAF catalogues, each window comprises 600 consecutive events. The corresponding overlap distance is 20 events for the nSAF and 30 events for the sSAF catalogues. The differences in window sizes and overlap distances are a necessary adaptation to the different number of events left in the declustered nSAF and sSAF catalogues respectively. In general, excellent approximations of the observed F-M-T distributions are obtained but for the sake of experimental rigour, this presentation will only consider models associated with a goodness of fit *better* than 0.97. The discussion focuses on the values and variation of the entropic indices, which are plotted as a function of time in Fig.5 and Fig 6 and summarized in Table 1.

Table 1. Summary of the entropic indices ans *b*-values obtained for the nSAF, sSAF and synthetic ETAS catalogues.

Parameter variation	Raw nSAF catalogue	Declustered nSAF catalogue	Raw sSAF catalogue	Declustered sSAF catalogue	Synthetic ETAS background based on sSAF
q_M	1.45 - 1.56	1.47 - 1.57	1.43 - 1.56	1.45 - 1.56	1.44 - 1.53 (in 5 runs)
q_T	1.06 – 1.69	1.26 - 1.65	1.01 - 1.98	1.39 - 1.78	1.19 - 1.00 (in 5 runs)
b_q	1.21 - 0.79	1.11 - 0.76	1.32 - 0.79	1.22 - 0.77	—
b (conventional)	—	1.1 - 0.78	—	1.25 - 0.86	—

As is apparent in Fig. 5, the analysis of the nSAF raw and declustered catalogues shows that the entropic index q_M, is quite consistently determined. For the raw nSAF catalogue, q_M generally varies between 1.56 and 1.45 (Fig. 5-top). It exhibits small fluctuations after the Loma Prieta main shock (M_L 7.0), first decreasing and, after approx. 1994, increasing slowly but persistently until the San Simeon and Parkfield earthquakes (M_L 6.6 and 6.0 respectively); a small increase can also be observed after approx. 2004.8. For the declustered nSAF catalogue q_M generally varies between 1.47 and 1.57 (Fig. 5-bottom); it exhibits a small but persistent increase before the Loma Prieta event and remains stable after 1989. The application of Eq. 9 leads to b_q estimates that vary from 0.79 to 1.21 for the raw catalogue and 0.76 to 1.11 for its declustered counterpart; it may be verified that these are remarkably consistent with corresponding determinations of *b*-values based on conventional methods (see Section 4.2 and Table 1). The entropic index q_M, like the *b*-value to which it is related, represents the scaling of the size distribution of earthquakes and clearly indicates a correlated, scale-free process, possibly exhibiting a small time dependence.

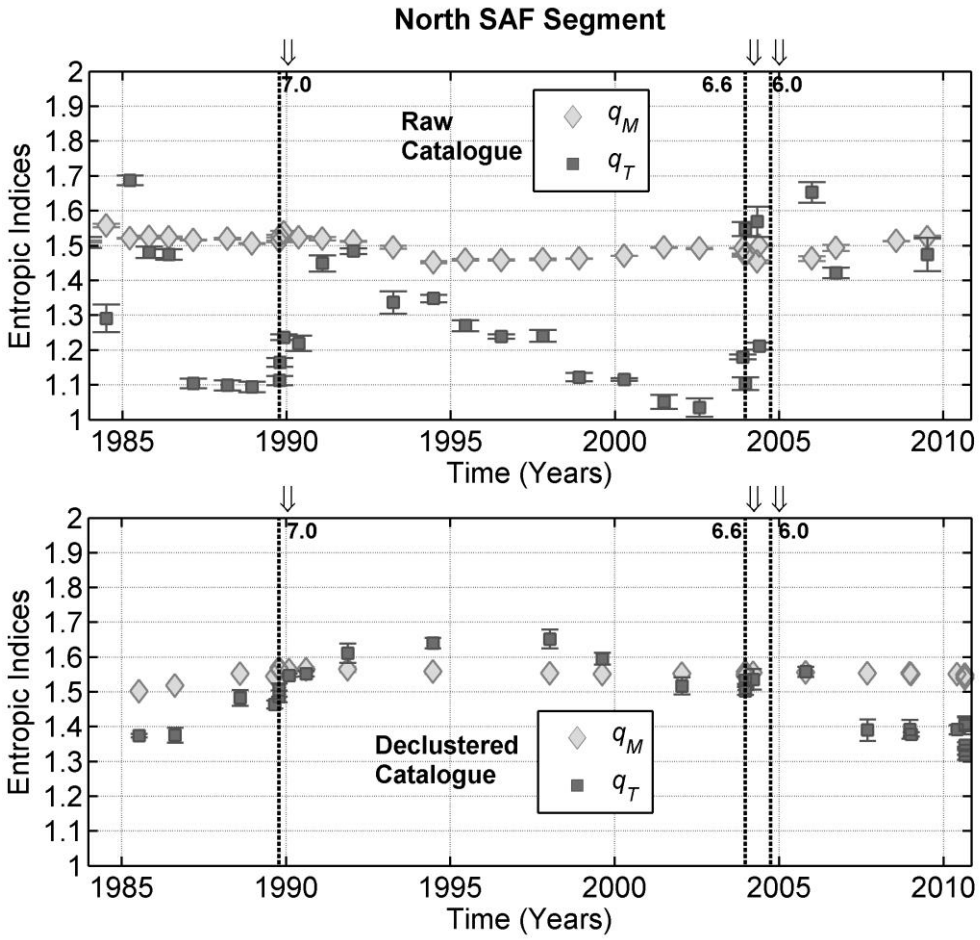

Figure 5. The entropic indices obtained for the raw (top) and stochastically declustered nSAF catalogues consisting of 1196 events with probability $\phi_j \geq 70\%$ to be background (bottom). Estimates are based on F-M-T distributions compiled over sliding windows of 450 events in the natural time of the seismogenetic process. Error bars refer to 95% confidence intervals. The vertical dashed lines indicate the occurrence of earthquakes with $M_L \geq 5.9$

The temporal entropic index q_T exhibits significant variation for both the raw and declustered catalogues. As can be seen in Fig. 5-top, for the raw nSAF catalogue and barring the period prior to year 1986 where it behaves erratically, q_T is generally low (< 1.2) prior to large earthquakes and attains significant values (> 1.4) immediately after their occurrence, indicating very high correlation that can be easily explained as a consequence of their aftershock sequences. This explanation is further corroborated by the observation that the high correlation observed after the 1989 Loma Prieta earthquake gradually decays to oblivion after year 2000, reaching a value of 1.04 which clearly indicates randomness. Conversely, the declustered nSAF catalogue reserves a surprise: q_T generally varies between 1.65 and 1.4, quasi-linearly increasing before the Loma Prieta earthquake from approx. 1.39 to 1.5 and remaining at high levels (> 1.5) up to year 2006; thereafter, it decreases to the level 1.3 – 1.4. In all cases moderate to high correlation is observed as a function of time indicating that the background process is *not* random at the 70% probability level.

The analysis of the raw and declustered sSAF catalogues also yields stable and consistent determination of q_M as a function of time. For the raw catalogue q_M varies between 1.43 and 1.56, exhibiting fluctuations that are localized in time and clearly associated with the occurrence of significant earthquakes (Fig. 6-top). For the declustered catalogue, q_M varies between 1.45 and 1.56, exhibiting small and slow variation with time, clearly not associated with significant events (Fig. 6-bottom). Respectively, b_q varies between 1.32 and 0.79 for the raw catalogue and between 1.22 and 0.77 for the declustered catalogue; these are also verifiably consistent with corresponding determinations of *b*-values based on conventional methods (Table 1).

The temporal entropic index exhibits intense variations with time. Fig. 6-top clearly shows that for the raw sSAF catalogue q_T behaves as per the raw nSAF catalogue; q_T is generally low (1.1 – 1.3) prior to large earthquakes but exhibits a persistent increasing trend from the lower to the higher end of this range prior to their occurrence; the index jumps to very high values (> 1.8) immediately after the incidence of large events, presumably reflecting the very high correlation associated with their aftershock sequences. Also as per the nSAF analysis, the high correlation of the aftershock sequences decays to near oblivion (< 1.1) with time, but a rate *significantly* faster than the corresponding effect associated with the Loma Prieta event (cf. Fig 5-top). Such behaviour indicates that quite different dynamics operate to the north and south of the Garlock Fault, as well as the possibility that nSAF seismicity is expressed with a series of rapidly building up and decaying cycles. The validity of these preliminary observations and inferences remains to be tested.

The analysis of the declustered sSAF catalogue holds its own surprises analogous to its nSAF counterpart: as shown in Fig. 6-bottom, q_T varies between 1.78 and 1.40. The entropic index is very high (> 1.7) up to the Landers event of 1992.5, slowly fluctuates to approx. 1.5 before the Hector Mine earthquake of 1999, decreases to approx. 1.4 by 2001, persistently increasing to 1.6 – 1.7 thereafter

and up to and after the Baja event of 2010. Such behaviour clearly indicates very high correlation for the background process and possibly SOC dynamics.

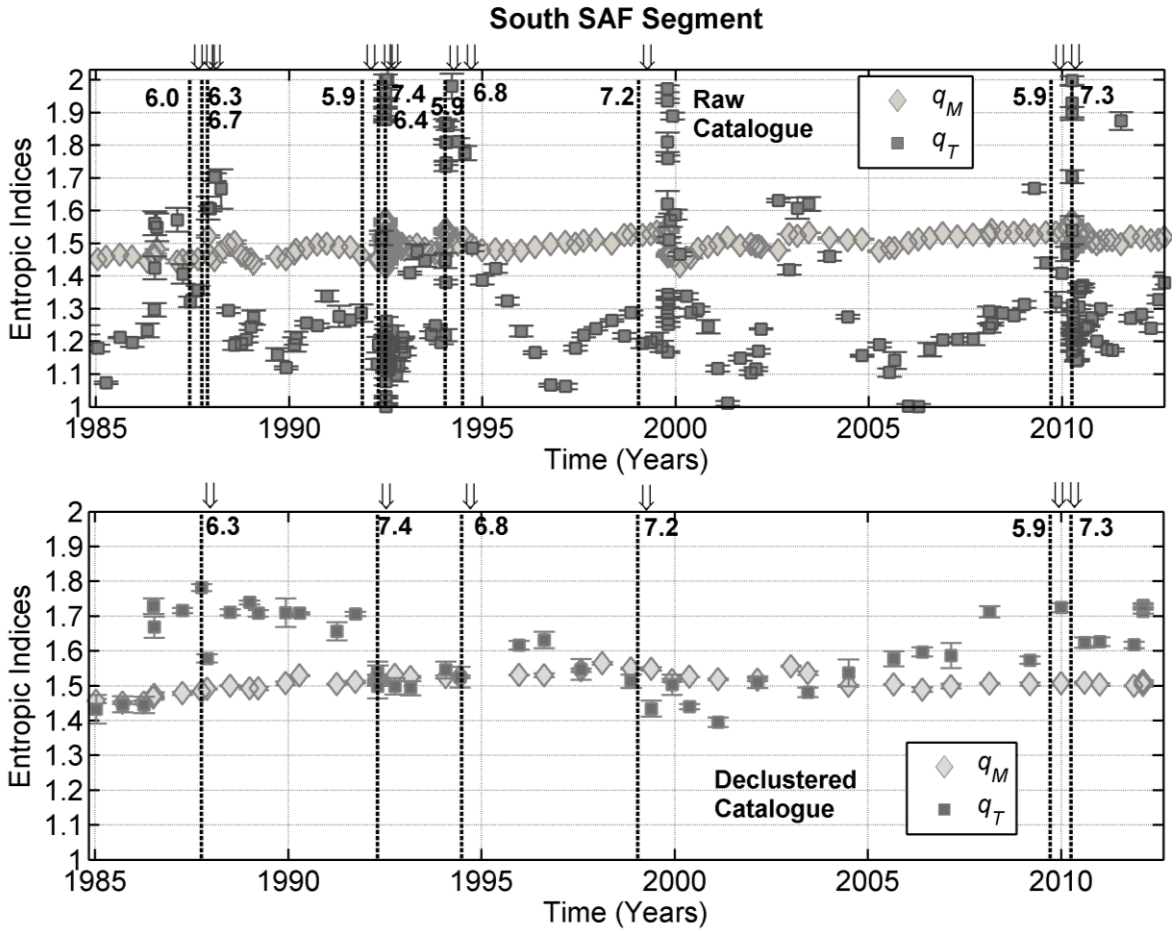

Figure 6. The entropic indices obtained for the raw (top) and a stochastically declustered sSAF catalogue consisting of 3200 events with probability $\phi_j \geq 70\%$ to be background (bottom). Estimates are based on F-M-T distributions compiled over sliding windows of 600 events. Error bars refer to 95% confidence intervals. The vertical dashed lines indicate the occurrence of earthquakes with $M_L \geq 5.9$

4.2 Validation tests

As stated at the end of Section 2, the level of similitude between b_q and b obtained with well-established methods of b-value estimation would be good indicator of the validity of the numerical estimation procedure used for the approximation of Eq. (8) and the robustness of the results and conclusions thereof. We test the performance of the estimation procedure by computing b as a function of time using robust weighted least squares and the same sliding window scheme as per Section 4.1. For the sake of brevity and clarity, we apply this analysis to the *declustered* nSAF and sSAF catalogues only. The results are compared with b_q in Fig. 7 and Table 1. It is apparent and that for the nSAF catalogue, b and b_q are practically identical. For the sSAF catalogue b and b_q exhibit very small differences in the interval 1997 – 2004 but are practically identical otherwise. The differences may, or

may not have physical meaning, but an explanation will not be sought herein. At any rate, the similitude between b_q and b is very high, indicating that Eq. (8) is solved with a rigorous and reliable estimation procedure.

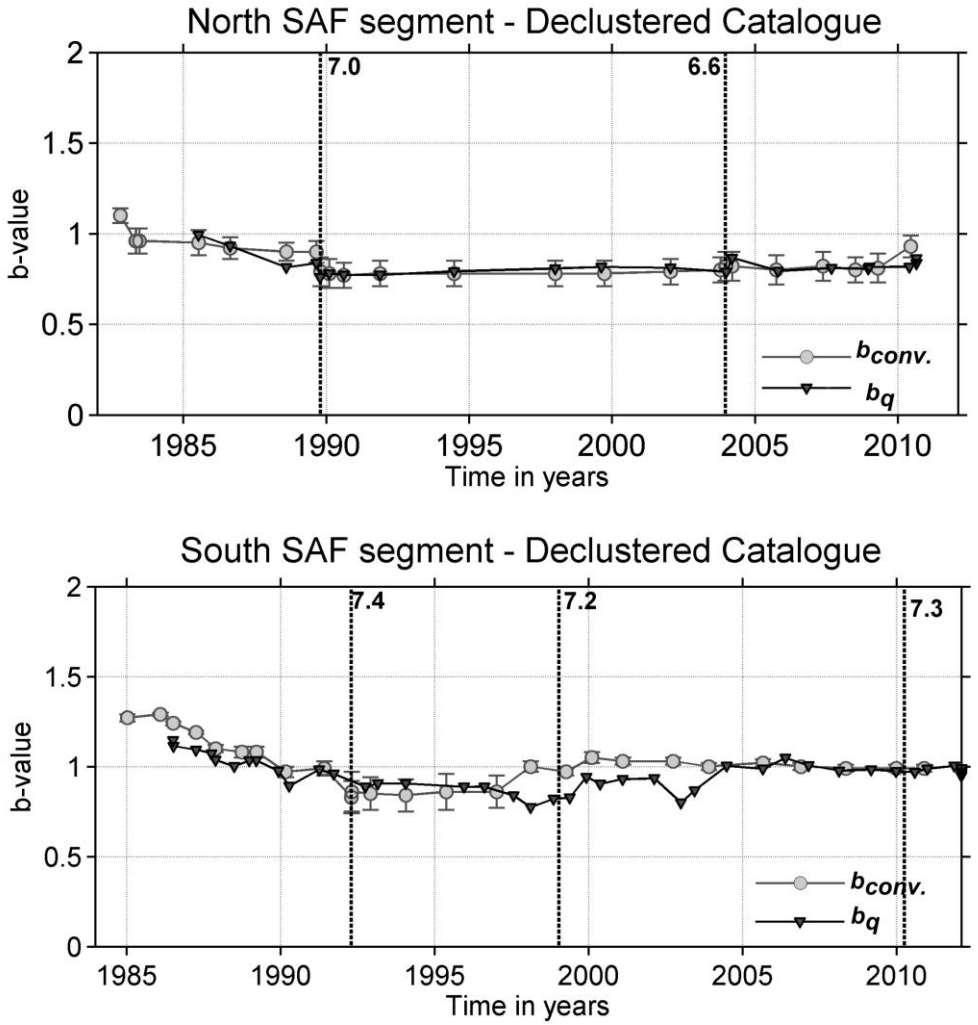

Figure 7. Comparison of b_q to conventionally estimated the b-values for the declustered nSAF (top) and sSAF (bottom) earthquake catalogues.

The analysis of the temporal entropic index presented in Section 4.1 above indicates that the "background" process along the SAF is not Poisson and, rather unexpectedly, exhibits stronger correlation than the mixed background – foreground process. A possible explanation s is deferred to Section 5 (Discussion). Nevertheless and to the extent that the results were obtained from catalogues declustered on the basis of the ETAS model, it is *absolutely necessary* to perform the same analysis on *several different* synthetic catalogues of background seismicity constructed on the basis of the ETAS model. This exercise will determine whether the results of Section 4.1 are significant and, presuming that the declustering procedure performed as intended, it will also define base values of the temporal entropic index q_T, above which it is safe to assume non-Poisson background processes.

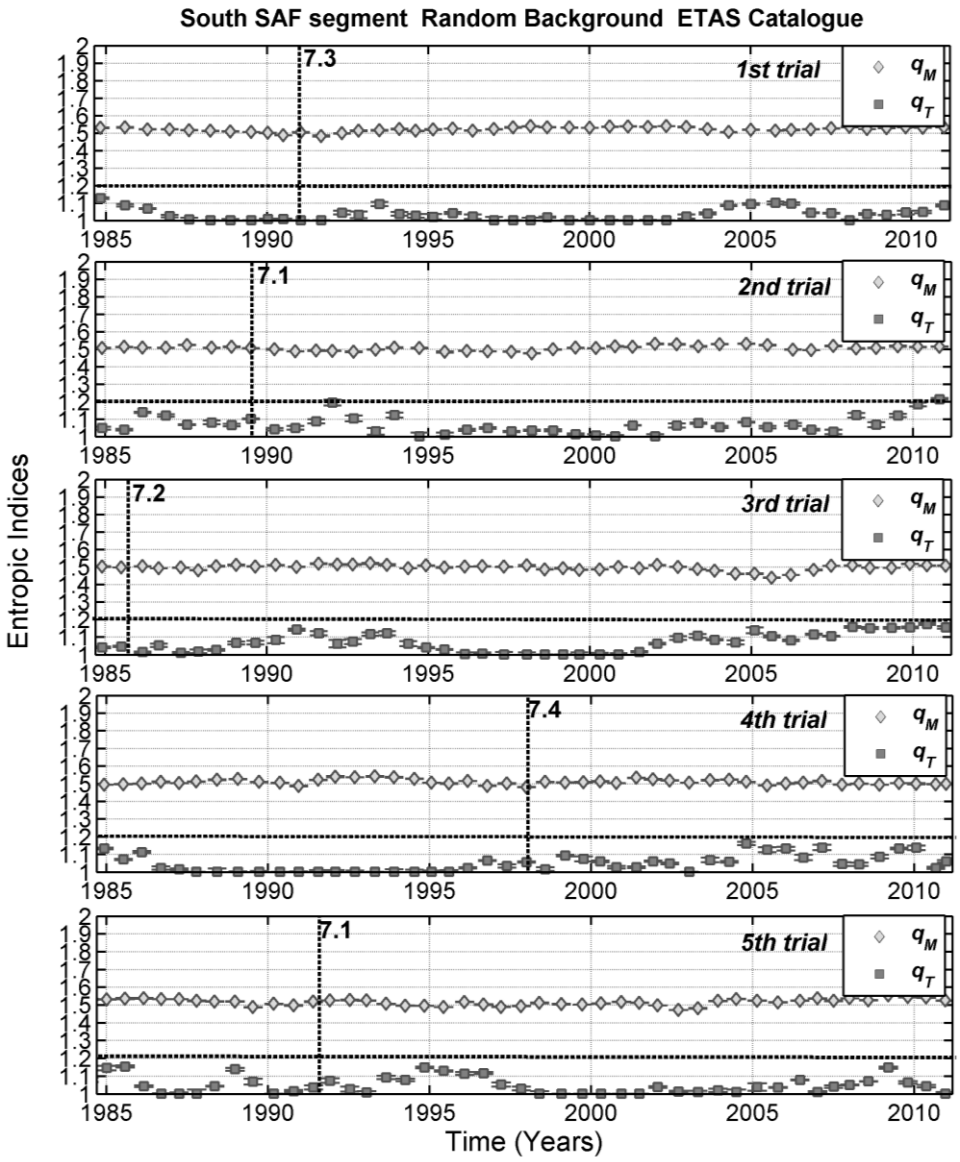

Figure 8. Analysis of five Synthetic ETAS background catalogues constructed with the characteristics of southern California seismicity. Estimates are based on F-M-T distributions compiled over sliding windows of 600 events with an overlap distance of 30 events. Error bars refer to 95% confidence intervals. The horizontal dashed line at q = 1.2 indicates the threshold above which the temporal entropic index q_T can be safely assumed to indicate non-Poissonian background.

Herein we use the stochastic ETAS aftershock simulator program "AFTsimulator" by Karen Felzer (2007), whose theoretical underpinning is detailed in Felzer et al, (2002) and Felzer and Brodsky (2006). The program uses empirical statistical laws of background and aftershock behaviour, and Monte Carlo methods to simulate background earthquakes and multiple generations of aftershocks. Known main shocks are input as point or planar sources and background earthquakes are chosen randomly from observed or contrived spatial distributions (grids) of earthquake rates. This facilitates the generation of realistic synthetic background catalogues, absolutely consistent with the known long-term seismotectonic characteristics of a given region. In order to be clear as possible about how the synthetic ETAS catalogues were generated, we have limited our analysis to southern California and

have adopted the ETAS parameterization discussed in Felzer (2008), as well as the main shock parameterization and background rates supplied with AFTsimulator for that region

In Fig. 8 we present the results of the application of the analytical procedure specified is Section 4.1 to five synthetic background catalogues compiled for the period 1980–2012, assuming only that the maximum expected magnitude is M_L = 7.4, (i.e. the observed maximum magnitude corresponding to the 1992 Landers event). It is apparent that q_M is stable and although it varies between the extreme values of 1.44 and 1.52, it basically fluctuates around a mean value of 1.5 (b_q = 1), without exhibiting systematic behaviour of some kind. Such behaviour is similar to that observed in the declustered sSAF catalogue. The expectation value of the temporal entropic index for point processes is unity. The experimental determination of q_T for the five synthetic ETAS catalogues indicates consistently low correlation in all cases, with the overwhelming majority of q_T determinations being consistently lower than 1.1 (practically random) and with max(q_T) < 1.2 throughout and without exception. Such behaviour of the q_T is very dissimilar to that observed for the declustered sSAF catalogue in Fig. 6 and because it is typical, it indicates that the systematic observation of empirical q_T values greater than 1.2 is compelling evidence of non-extensive dynamics.

5. Discussion and Conclusions

The present study is part of a systematic attempt to examine the nature of seismogenesis by searching for evidence of complexity and non-extensivity in accurate and reliable seismicity records. There are two general points of view as to the nature of the core (background) seismogenetic process: either it comprises a self-excited conditional Poisson process, or a (Self-Organized) Critical process. In the former case, core earthquakes are thought to be spontaneously generated in the seismogenetic continuum and are expected to be independent of each other. Accordingly, there should be no correlation between background events as there is no interaction between them and the thermodynamics of the process should obey the Boltzmann-Gibbs formalism. In the latter case, long-range interactions in non-equilibrium states are expected, so that background events should be correlated and the thermodynamics should deviate significantly from the Boltzmann-Gibbs formalism. Both points of view agree that the core earthquakes generate aftershock sequences (foreground earthquakes) which are genetically related to the parent event and comprise correlated sets. It follows that if were possible to identify and remove aftershocks, it would also be possible to investigate the nature of the seismogenetic system by examining background earthquakes for the existence of correlation.

Herein we search for correlation in the cumulative distributions of earthquake magnitudes and interevent (or waiting) times, in the context of non-extensive statistical physics, which has been developed by Tsallis (1988, 2009) as a generalization of Boltzmann-Gibbs dynamics to non-

equilibrating (non-extensive) systems. The search is performed on accurate, complete and homogeneous earthquake catalogues observed along the well-studied San Andreas Fault, California, U.S.A., in which aftershocks are either included or have been removed by an advanced stochastic declustering procedure (Zhuang et al, 2002, 2004). Moreover, it is based on the entropic indices associated with the NESP formalism (Section 2), which indicate the level on non-equilibrium or, equivalently, the extent of interaction and inter-dependence in a complex system. The entropic indices are computed over consecutive overlapping windows in the period 1980 – 2012 (function of time), so as to facilitate the study of time-dependence in the state of the faulting system along the SAF.

The entropic index associated with the distribution of magnitudes (q_M) generally varies about 1.5 and in the range 1.43 to 1.57 for both raw and declustered catalogues. Application of Eq. 9 yields a range of proxy-*b* values between 1.3 and 0.8, which is remarkably consistent with *b*-values computed with conventional (direct) means of estimation. In consequence, it is also consistent with the well-understood concept of scale-free organization in the size and geometry of the active tectonic grain along the SAF fault system, which can thus be classified as a *sub-extensive complex* with a high degree of self-organization.

More interesting observations can be made with regard to the temporal entropic index q_T, which conveys information about the dynamic state(s) of the system. Let us first focus on the analysis of the raw (measured) catalogues, which include both foreground and background processes. In both the nSAF and sSAF areas, q_T appears to shift from moderately to highly correlated states after the incidence and during the aftershock sequences of large earthquakes, to uncorrelated states as these die out and before the next large event. However, there is significant qualitative difference between the north and south stretches of SAF: Correlation is much stronger in the south ($q_T > 1.7$) immediately after large earthquakes, followed by relatively fast recovery to quasi-randomness, whereas it is appears to be weaker and decay at a significantly slower pace in the north. An additional difference is that in the south SAF, systematic return to a weak non-equilibrium (correlated) state is consistently observed prior to large events, with q_T gradually increasing from the level of 1.1 – 1.2 (uncorrelated) to approx. 1.3 and higher (weakly correlated). These differences may reflect changes in the mode of deformation between the southern and northern stretches of the SAF and their interpretation will be attempted elsewhere. Overall and at first sight, the temporal entropic index obtained from the raw nSAF and sSAF catalogues would appear to yield results consistent, or at least not conflicting, with the conclusions of numerous hitherto studies based on point process models. This would have been a valid conclusion, were it not for the declustered catalogues…

van Stiphout et al (1012) present comparisons of declustering algorithms in which they apply the χ^2 goodness of fit test to determine whether the background seismicity recovered by a given declustering algorithm obeys a Poisson distribution in time (null hypothesis). They found that at the 5% significance level, the methods of Zhuang et al. (2002) and Marsan and Lengliné (2008) follow a

Poisson distribution in time, although the corresponding estimated sets of background earthquakes differ considerably in absolute numbers. On these grounds, they appear to suggest that Poisson processes are in control of the background seismicity. We contend that this (and analogous) tests can be misleading because the distribution of occurrence times is *not at all* a measure of correlation between successive events and does not relate the occurrence of an earthquake to its predecessor and successor events. On the other hand, the distribution of interevent times does, as adequately explained in the foregoing. Accordingly, the analysis of the declustered catalogues clarifies that the "background" process exhibits moderate to high correlation with $q_T \in (1.35, 1.8]$ in general. Moreover, the correlation is not constant but varies considerably albeit *smoothly* with time. In the context of NESP, this would indicate that the background seismicity along the SAF expresses a persistent sub-extensive system whose entropy changes with time for physical reasons that are yet to be clarified. It is also apparent that the degree of correlation is overall higher in the sSAF than it is in the nSAF. In turn, this would indicate a considerably more unstable sSAF and would be consistent with the observation of shorter recurrence for large earthquakes in comparison to the nSAF.

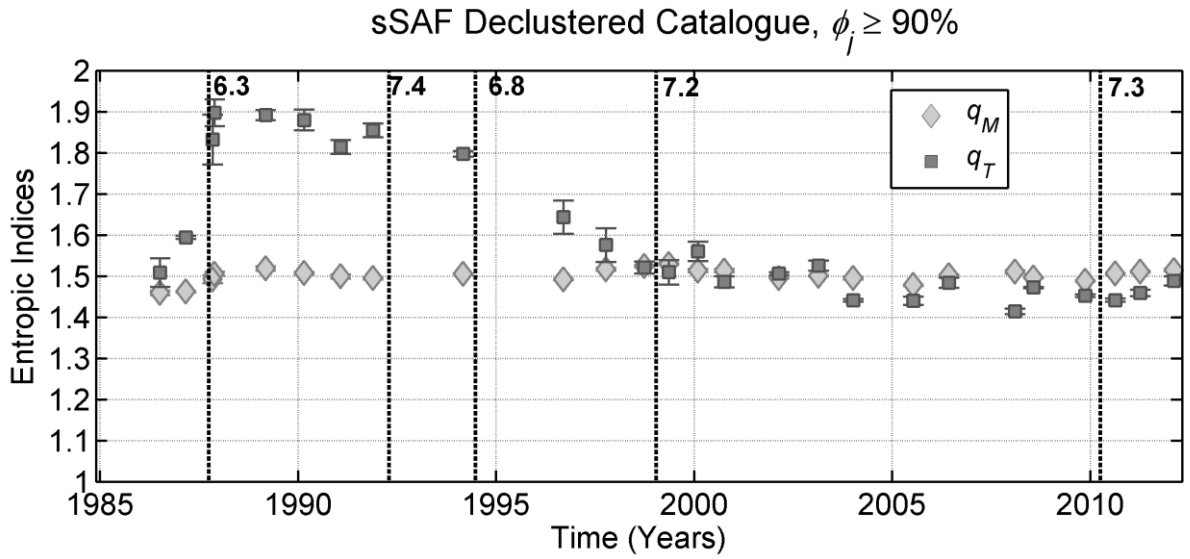

Figure 9. The entropic indices obtained for a stochastically declustered sSAF catalogue consisting of 1,724 events with probability $\phi_j \geq 90\%$ to be background. Estimates are based on F-M-T distributions compiled over sliding windows of 600 events. Error bars refer to 95% confidence intervals. The vertical dashed lines indicate the occurrence of earthquakes with $M_L \geq 6$.

A point of great significance is that by removing aftershock sequences, increased the correlation is observed throughout! However, it should be noted that because the declustered catalogues consist of events with probability $\phi_j > 70\%$ to be background, residual aftershocks are still present, as for instance can be observed for the aftermath of the M7, Loma Prieta earthquake of 1989 (Fig 5-bottom). It is straightforward to show that for higher ϕ_j thresholds, the results are qualitatively equivalent and quantitatively comparable. To emphasize this point, in Fig. 9 we present the analysis of a declustered

sSAF catalogue comprising 1,724 events with probability $\phi_j \geq 90\%$ to belong to the background, using the same windowing method as per Section 4.1. Clearly, the determination of q_M remains stable and its values are almost identical to the values determined for $\phi_j \geq 70\%$. The variation of q_T also remains the same in shape and time dependence, but q_T amplitudes are slightly higher prior to year 2000 by approx. 0.1 – 0.15 and slightly lower after year 2005 by approx. 0.1 as well! The differences are obviously related to the different content of the declustered catalogues and deserve further scrutiny. In any case, it is clear that on removing aftershock sequences, increased the correlation is observed throughout. Although this effect requires additional and rigorous experimental investigation, a plausible explanation is that because foreground processes are localized in time and space, their efficient removal unveils the existence of long-range interactions in the background process, which their presence otherwise obscures.

The results presented herein provide strong evidence of complexity in the expression of background seismicity along the San Andreas Fault. It goes without saying that supplementary experimental work and testing is required before the evidence becomes compelling. In addition, (SO) Criticality appears to a very likely explanation of the complexity mechanism, inasmuch as a persistent state of non-equilibrium can be inferred on the basis of the temporal entropic index and persistent fractal geometry is evident in the behaviour of the magnitude entropic index. However, conclusions cannot be drawn as yet! As discussed by Sornette and Werner (2009) in their comprehensive discussion, complexity may not only emerge from inherent non-linear dynamics of the active tectonic grain as required by SOC; quenched heterogeneity in the stress field and production rates may also be of great importance. It is also noteworthy that Celikoglu et al (2010) showed that it is possible to obtain *q*-exponential distributions of interevent times with models not involving criticality. Accordingly, additional work is required before mechanism of background seismicity can be proposed with confidence.

In a final comment, our results indicate that NESP is an excellent *natural* descriptor of earthquake statistics and appears to apply to the seismicity observed along the San Andreas Fault where sub-extensive thermodynamics appear to predominate. The NESP formalism, although far from having answered questions and debates on the statistical physics of earthquakes, appears to be an effective and insightful tool in the investigation of seismicity and its associated complexity.

Acknowledgments

We acknowledge insightful discussions with Dr M. Segou, particularly with respect to declustering. This work was partly supported by the THALES Program of the Ministry of Education of Greece and the European Union in the framework of the project "Integrated understanding of Seismicity, using innovative methodologies of Fracture Mechanics along with Earthquake and Non-Extensive Statistical Physics – Application to the geodynamic system of the Hellenic Arc - SEISMO FEAR HELLARC".

REFERENCES:

Abe, S., and N. Suzuki 2005. Scale-free statistics of time interval between successive earthquakes. *Physica A*, **350**, 588-596.

Bak, P. and C. Tang, 1989. Earthquakes as a self-organized critical phenomenon. *J. Geophys. Res.*, **94**, 15635-15637.

Bak, P., Christensen, K., Danon, L. and Scanlon, T., 2002. Unified scaling law for earthquakes, *Phys. Rev. Lett.*, **88**, 178501; doi:10.1103/PhysRevLett.88.178501.

Bakar, B. and Tirnakli, U., 2009. Analysis of self-organized criticality in Ehrenfest's dog-flea model, *Phys. Rev. E*, **79**, 040103; doi:10.1103/PhysRevE.79.040103.

Becker T.W., Hardebeck J.L. and Anderson G., 2005. Constraints on fault slip rates of the southern California plate boundary from GPS velocity and stress inversions, *Geophys. J. Int.*, **160** (2), 634–650.

Carbone, V., Sorriso-Valvo, L., Harabaglia, P. and Guerra, I., 2005. Unified scaling law for waiting times between seismic events, *Europhys. Lett.*, **71** (6), 1036; doi: 10.1209/epl/i2005-10185-0.

Caruso, F., Pluchino, A., Latora, V., Vinciguerra, S. and Rapisarda, A., 2007: Analysis of self-organized criticality in the Olami-Feder-Christensen model and in real earthquakes, *Phys. Rev. E*, **75**, 055101; doi: 10.1103/PhysRevE.75.055101.

Celikoglu, A., Tirnakli, U., and Duarte Queirós, S., 2010. Analysis of return distributions in the coherent noise model, *Phys. Rev. E*, **82**, 021124; doi:10.1103/PhysRevE.82.021124.

Corral, A., 2004. Long-term clustering, scaling, and universality in the temporal occurrence of earthquakes, *Phys. Rev. Lett.*, **92,** 108501.

Davidsen, J. and Goltz, C., 2004. Are seismic waiting time distributions universal? *Geophys. Res. Lett.*, **31**, L21612; doi 10.1029/2004GL020892.

Dengler, L., Moley, K., McPherson, R., Pasyanos, M., Dewey, J.W. and Murray, M.H., 1995. The September 1, 1994 Mendocino fault earthquake, *California Geology* **48**, 43 – 53.

Eaton J.P., 1992. Determination of amplitude and duration magnitudes and site residuals from short-period seismographs in Northern California, *Bull. Seism. Soc. Am.*, **82** (2), 533-579.

Felzer, K. R. and Brodsky, E. E. 2006 Evidence for dynamic aftershock triggering from earthquake densities, *Nature*, **441**, 735-738.

Felzer, K. R., 2007. Stochastic ETAS Aftershock Simulator Program (AFTsimulator), available at http://pasadena.wr.usgs.gov/office/kfelzer/AftSimulator.html; last access 20 October 2014.

Felzer, K. R., Becker, T. W., Abercrombie, R. E. , Ekstrom, G. and Rice J. R., 2002. Triggering of the 1999 Mw 7.1 Hector Mine earthquake by aftershocks of the 1992 Mw 7.3 Landers earthquake, *J. Geophys. Res.*, **107**, 2190; doi:10.1029/2001JB000911.

Felzer, K.R., 2008. Simulated aftershock sequences for a M 7.8 earthquake on the Southern San Andreas Fault, *Seism. Res. Lett.*, **80**, 21--25.

Fialko Y., 2006. Interseismic strain accumulation and the earthquake potential on the South San Andreas fault system, *Nature*, **441**; doi:10.1038/nature04797, 968-971.

Gardner, J. K., and Knopoff, L., 1974. Is the sequence of earthquakes in Southern California, with aftershocks removed, Poissonian? *Bull. Seism. Soc. Am.*, **64** (5), 1363-1367.

Gell-Mann, M. and Tsallis, C. (eds.), 2004. *Nonextensive Entropy – Interdisciplinary Applications*. Oxford University Press, New York.

Hainzl, S., Scherbaum, F. and Beauval, C., 2006. Estimating background activity based on interevent-time distribution, *Bull. Seismol. Soc Am.*, **96** (1), 313–320; doi: 10.1785/0120050053.

Hardebeck, J. L., and. Hauksson E., 2001. Crustal stress field in southern California and its implications for fault mechanics, *J. Geophys. Res.*, **106**, 21,859–21,882.

Hawkes, A.G. 1972. Spectra of some mutually exciting point processes with associated variables, in Stochastic Point Processes, P.A.W. Lewis (ed), Wiley, 261-271.

Hawkes, A.G. and Adamopoulos, L., 1973. Cluster models for earthquakes - regional comparisons, *Bull Internat. Stat. Inst.*, **45**, 454-461.

Hawkes, A.G. and Oakes, D., 1974. A cluster representation of a self-exciting process, *Journal Apl. Prob.*, **11**, 493-503.

Helmstetter, A. and Sornette, D., 2003. Predictability in the Epidemic-Type Aftershock Sequence model of interacting triggered seismicity, *J. Geophys. Res.*, **108** (B10), 2482; doi:10.1029/2003JB002485.

Jones L.M, 1989. Focal Mechanisms and the state of San Andreas Fault in Southern California, *J. Geophys. Res.*, **93** (B8), 8869-8891.

Marsan, D. and Lengliné, O., 2008. Extending earthquakes's reach through cascading, *Science*, **319**, 1076; doi: 10.1126/science.1148783.

Martinez, M.D., Lana, X., Posadas, A.M. and Pujades, L., 2005. Statistical distribution of elapsed times and distances of seismic events: the case of the Southern Spain seismic catalogue, *Nonlinear Proc. Geophys.*, **12**, 235–244.

Marzocchi, W. and Lombardi, A. M., 2008. A double branching model for earthquake occurrence, *J. Geophys. Res.*, **113**, B08317; doi:10.1029/2007JB005472.

Michas, G., Vallianatos,F. and Sammonds, P., 2013. Non-extensivity and long-range correlations in the earthquake activity at the West Corinth rift (Greece), *Nonlinear Proc. Geoph.*, **20**, 713-724.

Molchan, G., 2005. Interevent time distribution in seismicity: A theoretical approach, *Pure appl. geophys.*, **162**, 1135–1150; doi: 10.1007/s00024-004-2664-5.

Moré, J.J. and Sorensen, D.C., 1983. Computing a Trust Region Step, *SIAM Journal on Scientific and Statistical Computing*, **3**, 553–572.

Newman, M. E. J., 1996. Self-Organized Criticality, Evolution and the Fossil Extinction Record, *Proc. Roy. Soc. Lond. B*, **263**, 1605–1610.

Ogata, Y., 1988. Statistical models for earthquake occurrences and residual analysis for point processes, *J. Am. Stat. Assoc.*, **83** (401), 9-27.

Ogata, Y., 1998. Space-time point-process models for earthquake occurrences, *Ann. I. Stat. Math.*, **50** (2), 379-402.

Olami, Z., Feder, H. J. S. and Christensen, K., 1992. Self-Organized Criticality in a continuous, nonconservative cellular automaton modeling earthquakes, *Phys. Rev. Lett.*, **68**, 1244–1247.

Papadakis, G., Vallianatos, F. and Sammonds, P., 2013. Evidence of Nonextensive Statistical Physics behaviour of the Hellenic Subduction Zone seismicity, *Tectonophysics*, **608**, 1037-1048.

Reasenberg, P. 1985. Second-order moment of central California seismicity, 1969-82, *J. Geophys. Res.*, **90**, 5479, 5495.

Rhoades, D. A., 2007. Application of the EEPAS model to forecasting earthquakes of moderate magnitude in Southern California, *Seismol. Res. Lett.*, **78** (1), 110–115.

Rundle, J. B., Klein,W., Turcotte, D. L., and Malaud, B. D., 2000. Precursory seismic activation and critical point phenomena, *Pure appl. Geophys.*, **157**, 2165–2182.

Saichev, A. and Sornette, D., 2013. Fertility Heterogeneity as a Mechanism for Power Law Distributions of Recurrence Times, *Physical Review E*, **97**, 022815; also available at arXiv:1211.6062 [physics.geo-ph] (last access 20 October 2014).

Segou, M., T. Parsons, and W. Ellsworth, 2013. Comparative evaluation of physics-based and statistical forecasts in Northern California, *J. Geophys. Res. Solid Earth*, **118**, doi:10.1002/2013JB010313.

Silva, R., Franca, G.,S., Vilar, C.,S., Alcaniz, J.,S., 2006. Nonextensive models for earthquakes, *Physical Review E*, **73**, 026102; doi:10.1103/PhysRevE.73.026102.

Sornette, A. and Sornette, D., 1989. Self-organized criticality and earthquakes, *Europhys. Lett.*, **9**, 197-202.

Sornette, D. and Sammis, C. G., 1995. Complex critical exponents from renormalization group theory of earthquakes: Implications for earthquake predictions, *J. Phys. 1*, **5**, 607–619.

Sornette, D., and Werner, M.J., 2009. Statistical Physics Approaches to Seismicity, in Complexity in Earthquakes, Tsunamis, and Volcanoes, and Forecast, W.H.K. Lee (Ed), in the *Encyclopedia of Complexity and Systems Science*, R. Meyers (Editor-in-chief), 7872-7891, Springer, ISBN: 978-0-387-755888-6; available at arXiv:0803.3756v2 [physics.geo-ph] (last access 20 October 2014).

Sotolongo-Costa, O. and Posadas, A., 2004. Tsalli's entropy: A non-extensive frequency-magnitude distribution of earthquakes. *Phys. Rev. Letters*, **92** (4), 048501; doi:10.1103/PhysRevLett.92.048501.

Steihaug, T., 1983. The Conjugate Gradient Method and Trust Regions in Large Scale Optimization, *SIAM J. Numer. Anal.*, **20**, 626–637.

Talbi, A. and Yamazaki, F., 2010. A mixed model for earthquake interevent times, *J. Seismol*, **14**, 289–307; doi: 10.1007/s10950-009-9166-y.

Telesca, L., 2011. Tsallis-based nonextensive analysis of the Southern California seismicity. *Entropy*, **13**, 1267-1280.

Telesca, L., 2012. Maximum Likelihood Estimation of the Nonextensive Parameters of the Earthquake Cumulative Magnitude Distribution, *Bull. Seismol. Soc. Am.*, **102**, 886-891.

Touati, S., Naylor, M. and Main, I.G., 2009. Origin and Nonuniversality of the Earthquake Interevent Time Distribution, *Phys. Rev. Letters*, **102**, 168501; doi: 10.1103/PhysRevLett.102.168501

Tsallis, C., 1988. Possible generalization of Boltzmann-Gibbs statistics, *J. Stat. Phys.*, **52,** 479–487; doi:10.1007/BF01016429.

Tsallis, C., 2009. Introduction to Nonextensive Statistical Mechanics: Approaching a Complex World. Springer Verlag, Berlin, 378pp.

Uhrhammer B. R. A., Loper S. J., and Romanowicz B., 1996. Determination of local magnitude using BDSN Broadband Records, *Bull. Seism. Soc. Am.*, **86** (5), 1314-1330.

Utsu, T.; Ogata, Y.; Matsu'ura, R.S., 1995. The centenary of the Omori formula for a decay law of aftershock activity, *J. Phys. Earth*, **43**, 1–33.

Vallianatos, F., Benson, P., Meredith, P. and Sammonds, P., 2012. Experimental evidence of non-extensive statistical physics behaviour of fracture in triaxially deformed Etna basalt using acoustic emissions, *EPL-Europhys. Let.*, **97**, 58002.

Vallianatos, F. and Sammonds, P., 2013. Evidence of non-extensive statistical physics of the lithospheric instability approaching the 2004 Sumatran- Andaman and 2011 Honshu mega-earthquakes, *Tectonophysics*, doi: 10.1016/j.tecto.2013.01.009

Vallianatos, F. and Telesca, L. (Eds.), 2012. Statistical Mechanics in Earth Physics and Natural Hazards, *Acta Geophysica*, **60**, 499–501.

Vallianatos, F., Michas, G., Papadakis, G. and Tzanis, A., 2013. Evidence of non-extensivity in the seismicity observed during the 2011–2012 unrest at the Santorini volcanic complex, Greece. *Nat. Hazards Earth Syst. Sci.*, **13**, 177–185; doi:10.5194/nhess-13-177-2013.

van Stiphout, T., Zhuang J, and Marsan D., 2012, Seismicity declustering, Community Online Resource for Statistical Seismicity Analysis, doi: 10.5078/corssa-52382934. Available at http://www.corssa.org

Yeats R., 2013. *Active Faults of the World*, Cambridge University Press.

Zhuang J., Ogata Y. and Vere-Jones D., 2002. Stochastic declustering of space-time earthquake occurrences, *J. Amer. Stat. Assoc.*, **97**, 369-380.

Zhuang J., Ogata Y. and Vere-Jones D., 2004. Analyzing earthquake clustering features by using stochastic reconstruction, *J. Geophys. Res.*, **109** (B5), B05301; doi: 10.1029/2003JB002879.